Eur. J. Biochem. **269**, 3425–3432 (2002) © FEBS 2002 doi:10.1046/j.1432-1033.2002.03013.x

Fluorescent analogs of UDP-glucose and their use in characterizing substrate binding by toxin A from *Clostridium difficile*

Sudeep Bhattacharyya, Amy Kerzmann and Andrew L. Feig

Department of Chemistry, Indiana University, Bloomington, IN, USA

Uridine-5′-diphospho-1-α-D-glucose (UDP-Glc) is a common substrate used by glucosyltransferases, including certain bacterial toxins such as Toxins A and B from *Clostridium difficile*. Fluorescent analogs of UDP-Glc have been prepared for use in our studies of the clostridial toxins. These compounds are related to the methylanthraniloyl-ATP compounds commonly used to probe the chemistry of ATP-dependent enzymes. The reaction of excess methylisatoic anhydride with UDP-Glc in aqueous solution yields primarily the 2′ and 3′ isomers of methylanthraniloyl-UDP-Glc (MUG). As the 2′ and 3′ isomers readily interconvert, this isomeric mixture was copurified by HPLC away from the other isomeric products, and was characterized by a combination of NMR, fluorescence and mass spectrometric methods. TcdA binds MUG competitively with respect to UDP-Glc with an affinity of 15 ± 2 μM in the absence of Mg^{2+}. There is currently no evidence that the fluorescent substrate analog is turned over by the toxin in either glucosyltransferase or glucosylhydrolase reactions. Using a competition assay, the affinity of UDP-Glc was determined to be 45 ± 10 μM in the absence of Mg^{2+}. The binding of UDP-Glc and Mg^{2+} are highly coupled with Mg^{2+} affinities in the range of 90–600 μM, depending on the experimental conditions. These results imply that one of the significant roles of the metal ion might be to stabilize the enzyme–substrate complex prior to initiation of the transferase chemistry.

Keywords: fluorescence; *Clostridium difficile*; toxin A; UDP-glucose; glucosylhydrolase.

Clostridium difficile is a bacterium that causes antibiotic-associated diarrhea and pseudomembranous colitis [1–3]. Although *C. difficile* infection is widespread throughout the population, clinical manifestation of *C. difficile* associated diseases (CDAD) generally only occurs during antibiotic therapy due to the inability of this organism to compete against the other intestinal flora for nutrients [4]. *C. difficile* excretes two large toxins that have been linked to its pathogenicity, Toxin A (TcdA, P16154, molecular mass 308 kDa) and Toxin B (TcdB, P18177, molecular mass 270 kDa) [5]. Both toxins are glucosyltransferases and act upon the Rho subfamily of small GTPases (RhoA, Cdc42 and Ras) [6,7]. Glucosylation of these G-proteins at a key threonine residue initiates a cascade of events leading to actin filament depolymerization and, ultimately, cell-rounding and cell death [8,9]. The glucose donor for both toxins is UDP-glucose (UDP-Glc) [10]. In the absence of a suitable protein acceptor, the toxins catalyze the simple hydrolysis of UDP-Glc to UDP and free glucose (Scheme 1) [6,11].

The molecular biology and domain structure of these toxins has been studied previously [12,13]. TcdA and TcdB share 43% homology and 63% similarity and are members of a family of cytotoxins known as the large clostridial cytotoxins that also contains the lethal toxin from *C. sordellii* and the α-toxin from *C. novyi* [12]. Deletion experiments confirmed that the glucosyltransferase activity resides in an N-terminal domain of ≈ 660 amino acids [14]. The C-terminal domain, on the other hand, is responsible for interacting with a carbohydrate receptor on the surface of intestinal endothelial cells and cellular uptake of the toxin. A central hydrophobic region has been implicated in toxin escape from the endosome [15].

The catalytic domain of the toxin shares common features with a number of other glycosyltransferases. The nucleotide-binding region contains two conserved elements. The first is a tryptophan residue (W101 in TcdA) believed to assist in substrate recognition through interaction with the uridine group of UDP-Glc [16]. A second common feature to many glycosyltransferases is a DXD motif involved in binding a catalytically essential metal ion cofactor [17]. Comparative sequence alignments have identified D285 and D287 in TcdA as the aspartate residues of this motif [17]. Glycosyltransferases commonly employ Mg^{2+} and/or Mn^{2+} cofactors in their catalytic mechanisms and these toxins follow that paradigm [18]. Previous studies found the toxins to contain iron and zinc cofactors as well, but it is still unclear what role(s) these other cofactors might play [11]. Mechanistic studies of the glucosylhydrolase activity showed that Mg^{2+} or Mn^{2+} could stimulate activity and that K^+ also was required for enzyme activation [11].

Correspondence to A. Feig, Department of Chemistry, Indiana University, 800 E. Kirkwood Ave., Bloomington, IN 47405, USA, Fax: + 1 812 855 8300, Tel.: + 1 812 856 5449, E-mail: afeig@indiana.edu

Abbreviations: CDAD, *Clostridium difficile* associated disease; TcdA, *C. difficile* Toxin A; TcdB, *C. difficile* Toxin B; MeCN, acetonitrile; MUG, 2′/3′-methylanthraniloyl-uridine-5′-diphospho-1-α-D-glucose, BGT, T4 phage β-glucosyltransferase.

Proteins and enzymes: *C. difficile* toxin A (P16154); *C. difficile* toxin B (P18177); RhoA (P06749); Cdc42 (P25763).

Note: a website can be found at http://www.chem.indiana.edu/personnel/faculty/feig/feig.htm

(Received 15 February 2002, revised 14 May 2002, accepted 23 May 2002)

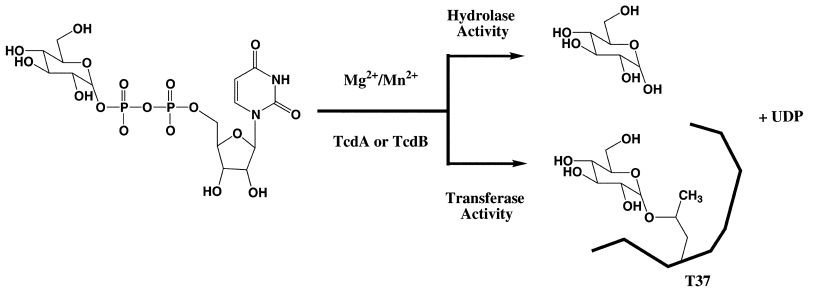

Scheme 1.

A common assay for the kinetic study of enzymatic UDP-Glc hydrolysis uses ^{14}C-nucleotide sugar complexes and employs anion exchange chromatography to separate the substrate and products [11]. This assay has been instrumental in studying the mechanism of glucosylhydrolase activity, but has several disadvantages, including the discontinuous nature of the data collection. We have therefore synthesized a series of fluorescent analogs of the nucleotide sugar complexes for use in studying glycosyltransferases in general and TcdA in particular. These substrate analogs are related to the commercially available methylanthraniloyl (mant) derivatives of ATP and GTP commonly used in mechanistic studies of ATPases and GTPases. Here, we report the synthesis, purification and characterization of methylanthraniloyl-UDP-Glc (MUG), and binding studies of this fluorophore to TcdA. We have also used this fluorophore to probe the interaction of TcdA with Mg^{2+} and UDP-Glc.

MATERIALS AND METHODS

Unless otherwise stated, all reagents were used without further purification. UDP-Glc, KCl, Hepes and dithiothreitol were purchased from Sigma. UDP-[U-^{14}C]glucose (320 mCi·mmol^{-1}) and [U-^{14}C]glucose (3 mCi·mmol^{-1}) were purchased from Amersham Pharmacia Biotech, USA. AG1-X2 ion exchange resin was obtained from Bio-Rad. Crude methylisatoic anhydride, obtained from Aldrich, was recrystallized twice from hot acetone prior to use. *C. difficile* toxin A (TcdA) was purchased from Tech Laboratory, Blacksburg, VA, USA. Solvents used for organic synthesis were reagent grade or better. Microcon filters with Ultracel-YM cellulose membranes (NMWL 10 000) were obtained from Millipore. RhoA and Cdc42 were prepared as GST fusion proteins, the clones for which were supplied by R. Cerione, Cornell University, Ithaca, NY, USA, and A. Bender, Indiana University, Bloomington, USA, respectively, and purified by affinity chromatography as previously described [19]. All buffers were prepared from the appropriate free acid and adjusted to the correct pH with KOH unless otherwise indicated.

Glucosylhydrolase activity assays

The glucosylhydrolase activity of TcdA was measured to ensure that the enzyme used in the spectroscopic studies was active. This assay is modeled after one previously reported by Ciesla & Bobak, but converted to batch mode [11]. In these studies, 100-μL reactions containing 50 mM Hepes pH 7.0, 150 mM KCl, 1 mM dithiothreitol, 100 μM UDP-Glc (2 mCi·mmol^{-1}), and 10 mM $MnCl_2$ were incubated in the presence or absence of TcdA (100 μg·mL^{-1}) at 37 °C. Aliquots (10 μL) were removed and quenched into 10 μL of 20 mM EDTA, pH 8.0. From this quenched reaction, 2 μL was set aside for determination of total counts while the remaining 18 μL were added to 150 μL of AG1-X2 resin beads (as a slurry made with 50 mM Hepes, pH 7.8) and 1 mL of 50 mM Hepes, pH 7.8. These samples were allowed to equilibrate at 4 °C on a rotary mixer and then the ion exchange resin was separated by centrifugation (2700 ***g*** for 15 s). The amount of product ([^{14}C]glucose) was then quantitated by liquid scintillation counting and the results are reported as the percent of the total counts in the quenched aliquot. Assays were typically run in triplicate and all data were corrected for the background hydrolysis of UDP-Glc in the absence of toxin. Inhibition studies were performed by varying the MUG and UDP-Glc concentrations and following the kinetics of the hydrolysis reaction.

Synthesis of MUG, a triethylammonium salt

This material was prepared essentially as described previously [20]. Briefly, 30 mg (0.05 mmol) of UDP-Glc was dissolved in 400 μL of distilled water and the pH of this solution was raised to 9.3 with 2 M NaOH solution. An excess of methylisatoic anhydride (30 mg, 0.17 mmol) was dissolved in 1.2 mL of dioxane and was added to the UDP-Glc solution. The suspension was stirred for 45 min at room temperature while being monitored by TLC (pre-Coated Plastic-Backed TLC sheets 250 μm, solvent system: NH_4OH/*n*-propanol/H_2O = 1 : 2 : 7, UV detection), and then filtered through a fritted glass disk. The solvent was removed from the filtrate under vacuum leaving an off-white solid. The crude product was resuspended in 800 μL of water, filtered though UNIFLO 0.45 μM syringe filters and stored at −20 °C pending purification.

The desired product was purified from the reaction mixture by reversed-phase HPLC by using a Beckman ultrasphere semipreparative (10 mm × 25 cm) C18 column installed in a Waters 600 gradient controller and connected to a Waters 2486 dual-wavelength absorbance detector and a fraction collector. A triethylammonium/acetate buffer system was used together with an acetonitrile gradient for the HPLC purification. Buffer A consisted of 10 mM triethylammonium/acetate (10 mM triethylamine in water adjusted to pH 5.5 with acetic acid) whereas buffer B was 10 mM triethylammonium/acetate, pH 5.5 in 90% MeCN. Purification was achieved with a four-step gradient program: 0–5 min, 94 : 6 (%A/%B); 5–13 min, linear gradient to 55 : 45; 13–50 min, linear gradient to 45 : 55; 50–75 min, linear gradient to 0 : 100. Products were detected by simultaneous monitoring at A_{260} and A_{330},

and the 2′/3′ mixture eluted at a retention time of ≈ 15 min. Solvents from the eluted fractions were removed under reduced pressure without heating. The final purified yield was 10 mg (20%). A 10 mM stock solution of this product was prepared; the pH was adjusted to 6.5, and the material was stored at −20 °C. The purified product was characterized by NMR: 2′-MUG ^{1}H-NMR (D_2O): δ = 6.5–8.0 (m, 4H, Ar-H), 5.8–6.1 (m, 1H, H-1′), 5.3–5.5 (m, 2H, H-1′, H-5), 4.4–4.6 (m, 1H, H-2′), 4.0–4.3 (m, 3H, H-3′, H-4′, H-5′), 3.5–3.8 (m, 3H, H-3′, H-5′, H-6′), 3.2–3.4 (m, 2H, H-2′, H-4′), 2.75 (s, 1H, N-CH_3); 3′-MUG ^{1}H-NMR (D_2O): δ = 7.8–8.0 (2H, Ar-H, H-6), 7.35–7.45 (1H, Ar-H), 6.65–6.80 (1H, Ar-H), 6.55–6.65 (1H, Ar-H), 6.05 (d,1H, H-1′), 5.7–5.8 (1H, H-5), 5.3–5.5 (2H, H-3′, H-1′), 4.4–4.6 (2H, H-2′, H-4′), 4.0–4.3 (2H, H5′), 3.5–3.8 (4H, H-3′, H-5′, H-6′), 3.2–3.4 (2H, H-2′, H-4′), 2.75 (s, 3H, N-CH_3); ^{31}P-NMR (D_2O):δ = −10.8 (d, 1P, αP); −12.5 (d, 1P, βP). MALDI-TOF mass spectrometry, UV/Vis and fluorescence further verified that we had the appropriate material: MS (MALDI-TOF matrix: 2,5-dihydroxybenzoic acid) m/z = 697.8 (calc. M^{2-} = 697.4). UV(D_2O) λ(absorption) = 358 nm (ε = 1500 $M^{-1}\cdot cm^{-1}$). Fluorescence: λ_{ex} = 358 nm, λ_{em} = 440 nm. At equilibrium (25 °C), the 2′/3′ isomer ratio is approximately 1 : 1.2 based on integration of the NMR signal derived from the *N*-methyl groups of the methylanthraniloyl group.

Enzyme manipulation

Initial toxin stocks were prepared phosphate-buffered saline at concentrations of 1.0–1.35 $mg\cdot mL^{-1}$ and analyzed by SDS/PAGE to ensure homogeneity. Buffer exchange was performed at 4 °C by three cycles of 10-fold concentration in Microcon filter units (Ultracel-YM cellulose membrane, NMWL 10 000) and re-dilution into the assay buffer, after which the protein containing retentate was removed from the filtration unit. For spectroscopic studies that required high concentrations of toxin, the protein was left in its concentrated form after the final centrifugation step. Subsequent protein concentrations were measured by using the Bio-Rad Protein Assay following the manufacturer's protocol standardized against BSA. Typically, greater than 90% of the toxin was recovered after buffer exchange and concentration.

Fluorescence measurements

All fluorescence measurements were performed in a Perkin-Elmer LS50B luminescence spectrometer using microvolume fluorescence cuvettes. Initial studies of MUG fluorescence were performed at 50 nM MUG in 50 mM Hepes, pH 7.6 and 150 mM KCl. Binding titrations were performed in solutions containing 50 nM MUG in 50 mM Hepes, pH 7.6, 150 mM KCl, and 1 mM dithiothreitol. Under these conditions, the fluorescence intensity of free MUG was negligible compared to that of the enzyme complex. During these titrations, the concentration of MUG was held constant while the concentration of the toxin was varied between 0 and 28.4 μM. The initial sample contained 28.4 μM TcdA. This sample was then serially diluted with a buffer containing all components except the toxin to avoid dilution artifacts. Samples were equilibrated for 10 min at 4 °C after which time, the fluorescence intensities were measured and averaged over five scans. Data were analyzed by nonlinear least squares curve-fitting to standard binding isotherms by using the program KALEIDAGRAPH (Synergy Software). Similar titration strategies were used to obtain data over a wide range of Mg^{2+} concentrations without dilution of either the toxin or the fluorophore.

Competitive binding between MUG and UDP-Glc was observed under similar experimental conditions. Solutions of 50 nM MUG and 0.4 μM TcdA in 50 mM Hepes, pH 7.6 and 150 mM KCl containing varying concentrations of UDP-Glc (0–145 mM) were studied. The variable concentrations of UDP-Glc were obtained by starting with a stock solution containing all of the components including 145 mM UDP-Glc. This solution was then serially diluted with a second solution, identical to the first, except that it contained no UDP-Glc. Samples were mixed manually in the cuvettes at 4 °C and allowed to equilibrate for 10 min prior to analysis of MUG fluorescence emission at 440 nm (358 nm excitation). As the metal ion cofactor is missing from these samples, no significant toxin-catalyzed UDP-Glc hydrolysis should have occurred during these experiments.

RESULTS AND DISCUSSION

Synthesis of fluorescent UDP-Glc analogs

The methylanthraniloyl derivatives of nucleotides such as ATP and GTP have been used extensively as fluorescent analogs in the study of nucleotide binding sites on proteins [21–23]. Surprisingly, however, the related compounds have not been used to probe enzymes that use nucleotide diphosphate sugars complexes. The synthesis of the fluorescently-labeled UDP-Glc was carried out by modifying a preparative method for similar molecules, as described previously [20]. The coupling was achieved by combining a stoichiometric excess of methylisatoic anhydride with a solution of UDP-Glc held at pH 9.3. The reaction between ribose sugar alcoholic group(s) with the anhydride yields the desired product (Scheme 2) together with several isomeric byproducts. The 2′, 3′ and 6″ modified UDP-Glc were the dominant products of the reaction, as predicted from previous computational studies [20]. This differential reactivity made it unnecessary to protect the glucose moiety prior to derivatization, thus providing an extremely simple and efficient route to these substrate analogs.

Reverse-phase HPLC purification resolved the isomers present in the reaction mixture. The major fractions were subsequently identified by NMR analysis. The differential reactivity predicted in the previously mentioned study [20] was observed, showing three major isomers of the desired MUG, due to 2′- and 3′- and 6″-ester products. In solution, the 2′- and 3′-derivatives readily interconvert with each other resulting in an equilibrium mixture (1 : 1.2 ratio at 25 °C) of these two products after purification. In the case of mant-ATP and mant-GTP, the 2′ and 3′ isomers can sometimes be resolved and used independently prior to re-equilibration [24–27]. Such experiments are possible with MUG, but no attempt was made to achieve this level of separation. The purified reaction product was stable in aqueous solution at moderate pH (6–7) and was stored as a 10 mM stock solution (pH 6.5) at −20 °C.

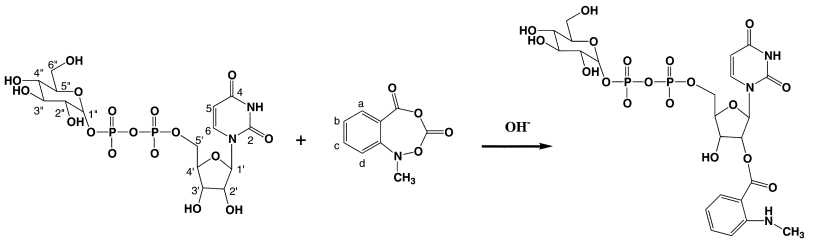

Scheme 2.

Toxin activity studies

Toxin activity was verified by using several kinetic assays, including a procedure modeled after the studies of Ciesla & Bobak [11]. They employed an assay based on ion exchange chromatography to separate unreacted UDP-[U-^{14}C]Glc and UDP from [U-^{14}C]Glc followed by quantitation by scintillation counting. Our assay is fundamentally the same except that it uses a batch mode format to facilitate working with many samples simultaneously. In these studies, TcdA was capable of turning over at a rate of 32 ± 3 (mol UDP-Glc)·(mol TcdA)$^{-1}$·h^{-1} under our standard conditions (Scheme 1). Our activities were slightly higher than that reported previously [19 (mol UDP-Glc)·(mol TcdA)$^{-1}$·h^{-1} under similar conditions], but the results are otherwise quite comparable [11]. Similar studies employing ^{31}P-NMR that follow the formation of UDP also allowed determination of glucosylhydrolase activity by UDP-Glc (data not shown). This latter assay was useful for assessing whether the enzyme could turnover the substrate analog without resorting to the synthesis of methylanthraniloyl-modified UDP-[U-^{14}C]Glc. No evidence for glucosylhydrolase activity of MUG was detected (probed out to 5 days). Furthermore, MUG acts as a very weak competitive inhibitor ($K_i = 400 \pm 100$ μM at 37 °C) with respect to UDP-Glc.

Florescence properties of MUG and the TcdA–MUG complex

The excitation and emission spectra of MUG are shown in Fig. 1A. As expected, this compound is highly fluorescent and yields excitation and emission spectra quite similar to the parent mant-ATP compound after which it was modeled [21]. Binding of MUG to TcdA leads to significant changes in the emission spectrum (Fig. 1B). The fluorescence intensity of the 50 nM MUG solution increases more than 20-fold upon binding to TcdA. In addition, the emission maximum undergoes a 10-nm blue shift. Finally, the transition at 410 nm in the emission spectrum is obscured by the dominant 440 nm peak in the spectrum of the protein-bound MUG. When RhoA or Cdc42 are added to solutions of MUG in the absence of TcdA, no spectral changes are observed. Therefore, the observed fluorescence changes are the result of a specific interaction between the substrate analog and the toxin. These spectral differences provide a convenient handle with which to measure the affinity of the toxin for the fluorescent substrate analog (K_{MUG}).

In the presence of a fixed concentration of MUG, TcdA was titrated into the sample in great excess of the

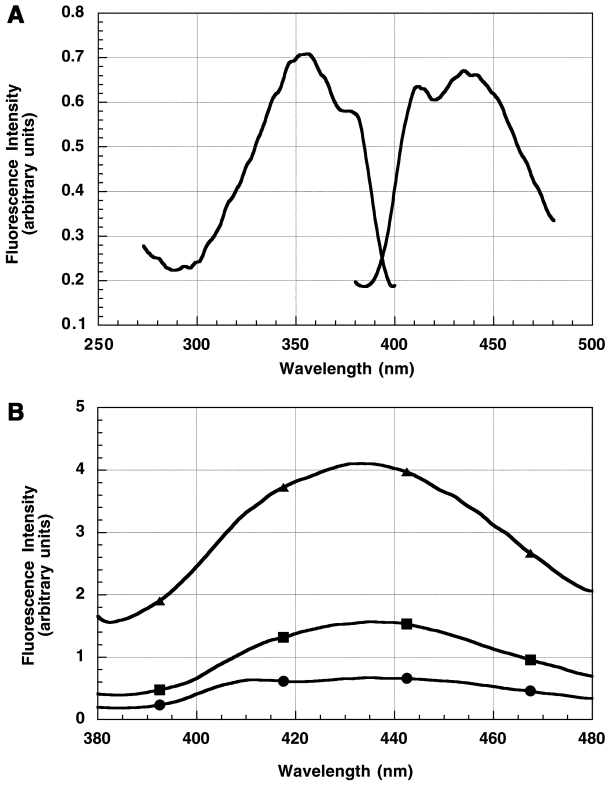

Fig. 1. Relative fluorescent intensity of MUG. (A) Excitation and emission spectra of 50 nM MUG in 50 mM Hepes, pH 7.6, 150 mM KCl, 1 mM dithiothreitol. (B) Fluorescence emission spectra of 50 nM MUG alone (●) or in the presence of 0.4 μM TcdA (■) or 0.4 μM TcdA and 10 mM $MgCl_2$ (▲). All three samples were prepared in 50 mM Hepes, pH 7.6, 150 mM KCl, 1 mM dithiothreitol. The excitation scan was collected while monitoring emission at 440 nm and emission data were collected with 358 nm excitation.

fluorophore (Fig. 2). This methodology avoids potential complications due to changes in the concentration of the fluorophore and hence simplifies the data analysis. These studies showed that MUG binds to the toxin with an affinity of 15 ± 2 μM at 4 °C. The 15 μM binding affinity is similar in magnitude to the 6 μM K_d measured for UDP-Glc binding to the related *C. sordellii* lethal toxin (catalytic domain) at 25 °C by intrinsic fluorescence [28]. The affinity of the modified substrate is therefore well within the range one might expect for binding to the natural substrate. Due to the large size of the holotoxin and the numerous tryptophan residues, intrinsic fluorescence experiments to

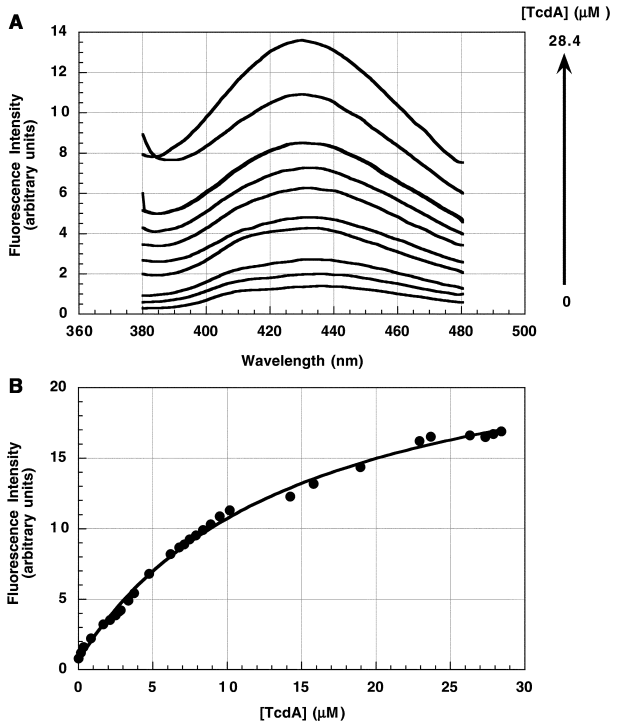

Fig. 2. MUG fluorescence in the presence of TcdA. (A) Titration of 50 nM MUG with TcdA (0–28.4 μM) monitored by fluorescence emission. Experimental conditions: 50 mM Hepes, pH 7.6, 150 mM KCl, 1 mM dithiothreitol, 4 °C, $\lambda_{ex} = 358$ nm, $\lambda_{em} = 440$ nm; (B) Plot of fluorescence intensity vs. [TcdA] fit to a standard binding isotherm. Experimental conditions: 50 nM MUG, buffer 150 mM KCl, 50 mM Hepes, pH 7.6, 1 mM dithiothreitol, 4 °C, $\lambda_{ex} = 358$ nm, $\lambda_{em} = 440$ nm.

look at the binding of the natural UDP-Glc substrate were not attempted.

Competitive binding studies were performed with the natural UDP-Glc substrate to ensure that binding occurred in the active site. Addition of UDP-Glc to the MUG–TcdA complex results in a decrease of fluorescent intensity due to displacement of MUG from the active site (Fig. 3). This

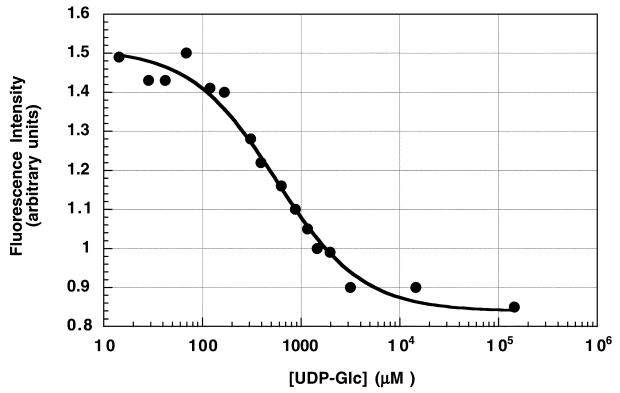

Fig. 3. Plot showing the decrease in relative fluorescence intensity of MUG (50 nM) bound TcdA (0.43 μM) upon addition of UDP-Glc (0–145 mM). Experimental conditions: 50 mM Hepes, pH 7.6, 150 mM KCl, 1 mM dithiothreitol, 4 °C, $\lambda_{ex} = 358$ nm, $\lambda_{em} = 440$ nm.

finding corroborates the fact that these molecules bind in competitive fashion in the active site pocket and probes the equilibrium constant ${}^{MUG}K_{UDP\text{-}Glc}$. A plot of the fluorescence intensity vs. [UDP-Glc] can therefore provide information on the affinity of UDP-Glc for the toxin, expressed as the ratio of the two dissociation constants. As the K_{MUG} value was measured independently, we can estimate the apparent affinity of the toxin for UDP-Glc ($K_{UDP\text{-}Glc}$), yielding a value of 45 ± 10 μM. This value is about threefold lower than the K_m value (142 μM) that has been measured under similar conditions with the exception that Mg^{2+} was present in the kinetics measurement [11].

Two oddities derive from the analysis of these data. The first is that in the absence of Mg^{2+}, MUG actually binds more tightly than UDP-Glc. This increased affinity almost certainly comes from additional hydrophobic interactions in the active site due to the large methylanthraniloyl group that is being sequestered. It should be noted that this binding is being monitored in the absence of the Mg^{2+}/Mn^{2+} cofactors. On the other hand, the inhibition data mentioned above ($K_i = 400$ μM) showed that MUG is a rather poor competitive inhibitor; data collected in the presence of saturating concentrations of the metal cofactor. Together, these data are indicative of two modes of substrate binding (i.e. open and closed). The closed, active form of UDP-Glc binding is only observed in the presence of the metal ion that properly aligns the UDP-Glc in the active site. The unfavorable steric interactions deriving from the presence of the fluorescent tag on the ribose 2′/3′ position might preclude proper orientation in the tight binding (closed) and catalytically active conformation. Therefore, we began to probe the affect metal binding on substrate affinity.

The initial fluorescence studies were performed in the absence of either Mg^{2+} or Mn^{2+}, but enzyme activity requires one or both of these ions to be present. The addition of Mg^{2+} up to 10 mM concentration has a significant effect on the fluorescence intensity of the TcdA–MUG complex, allowing us to probe the interaction between the metal cofactor and the TcdA–MUG complex. In the absence of TcdA, the addition of Mg^{2+} has no effect on the fluorescence intensity of MUG, so the change in fluorescence is a result of forming the TcdA–MUG–Mg^{2+} ternary complex. A titration curve for the binding of Mg^{2+} to the TcdA–MUG complex is shown in Fig. 4, yielding an apparent affinity (${}^{MUG}K_{Mg}$) of 90 ± 10 μM for the metal ion cofactor in the presence of 0.4 μM TcdA. Scatchard analysis of the data shows no indication of additional complexities such as multiple binding sites. When this experiment is repeated in the presence of higher concentrations of TcdA, the apparent affinity for Mg^{2+} decreases significantly with an affinity of 600 μM measured at 2 μM TcdA. The real affinity is probably even slightly weaker than that, as the 2 μM concentration of TcdA was insufficient to saturate MUG binding.

Based on our data, we can draw a thermodynamic cycle that represents the binding of TcdA to MUG, UDP-Glc and Mg^{2+}. This cycle is shown in Fig. 5. In the simplest case, one might have expected independent binding of Mg^{2+} and MUG(UDP-Glc) to TcdA. This statement is equivalent to saying that ${}^{UDP\text{-}Glc}K_{Mg} = {}^{MUG}K_{Mg} = K_{Mg}$, as defined in Fig. 5. Two outcomes to that argument must also be true in the case of independent binding: $K_{MUG} = {}^{Mg}K_{MUG}$ and $K_{UDP\text{-}Glc} = {}^{Mg}K_{UDP\text{-}Glc}$. Had this

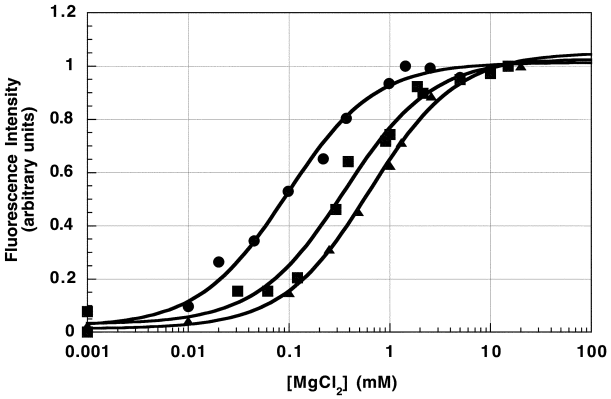

Fig. 4. Plot of the fluorescence intensity vs. $MgCl_2$ concentration at 0.4 (●), 0.8 (■) and 2.0 (▲) μM TcdA in the presence of 50 mM MUG, 150 mM KCl, 50 mM Hepes, pH 7.6 and 1 mM dithiothreitol at 4 °C, λ_{ex} = 358 nm, λ_{em} = 440 nm. Data were fit to standard binding isotherms yielding apparent affinities of 100 ± 15, 350 ± 50, 630 ± 40 μM, respectively.

been the case, we would have measured the same Mg^{2+} affinity regardless of the TcdA concentrations, as the metal binding event would be totally independent of the interactions involved in the enzyme–substrate complex. The binding of MUG and Mg^{2+} are not independent, however, but instead are highly coupled to one another. It is likely that by analogy, there is coupled binding between the metal ion cofactor and the natural UDP-Glc substrate. Magnesium appears to bind more weakly to the TcdA–MUG complex than to free TcdA ($K_{Mg} \leq 90$ μM, whereas ${}^{MUG}K_{Mg} \geq 600$ μM). Using the limits obtained in the experiment shown in Fig. 4 and the thermodynamic cycle in Fig. 5, we can set the limit that ${}^{Mg}K_{MUG} \leq 100$ μM. These data suggest that an ordered mechanism is involved in the reaction chemistry, a feature that can be assessed in future studies through detailed kinetic analysis of the hydrolase and transferase reactions.

Previous studies showed the importance of the metal ion cofactor for activity, but provided only an upper limit (< 2 mM) on the actual affinity [11]. In that study, they also showed that the K_m for UDP-Glc was weakly affected by binding of the metal ion cofactor. In our studies, the thermodynamic cycle lets us define a lower limit of 1 mM for the affinity of the TcdA–UDP–Glc complex for Mg^{2+}. Thus, the Mg^{2+} affinity is now narrowly bound by these two studies. The thermodynamic scheme presented in Fig. 5 is fully consistent with the data of Ciesla & Bobak [11] as well as that presented here. The main interpretation of this thermodynamic scheme is that the presence of the metal cofactor helps maintain the integrity and stability of enzyme–substrate complex. It is therefore likely that the ion simultaneously interacts with both the enzyme and UDP-Glc in the active site and that the glucosyl donor becomes realigned in the active site as a result of its contacts with the Mg^{2+} cofactor, thus affecting its affinity.

One major difficulty commonly encountered in studying Mg-dependent enzymes is the lack of convenient spectroscopic handles that can be used to probe directly the Mg^{2+} binding to TcdA [29]. Mg^{2+} binding to free TcdA is invisible to our assays. Thus, in this study, we have resorted to looking at the effects of Mg^{2+} binding on the other relevant equilibria. On-going studies using Mn^{2+} EPR methods and phosphorothioate derivatives of UDP-Glc will allow another look at these coupled processes and provide further details on the interaction of UDP-Glc, TcdA and the metal ion cofactor.

In vivo, TcdA catalyzes the transfer of glucose from UDP-Glc to a threonine residue of its acceptor protein (Scheme 1). The affinities of TcdA for these acceptors have not been measured carefully, but kinetic studies show efficient glucosyl transfer in the presence of 1 μM acceptor. Addition of either GST–Cdc42 or GST–RhoA (up to 1.5 μM) induced only minor changes in the fluorescence spectrum. It is therefore not practical to measure the affinities of the acceptor using MUG fluorescence. The most likely reason for this result is that the binding of the acceptor does not significantly alter the environment around the methylanthraniloyl group that is already protected from solvent in the TcdA–MUG complex.

Comparison of the UDP-Glc binding pockets of several structurally characterized glycosyltransferases, such as SpsA *Bacillus subtilis* [30], LgtC from *Neisseria meningitidis* [31], T4 bacteriophage DNA β-glucosyltransferases (BGT) [32,33] and UDP-galactose:β-galactosyl α-1,3-galactosyltransferase (α3GT) [34], supports the idea that the glucose acceptor might have only relatively minor effects on the environment around the donor. In each case, the nucleotide portion of the substrate is buried deep within the transferase active site. A channel or cleft is available for the acceptor to approach the glycosyl donor involved in the transferase

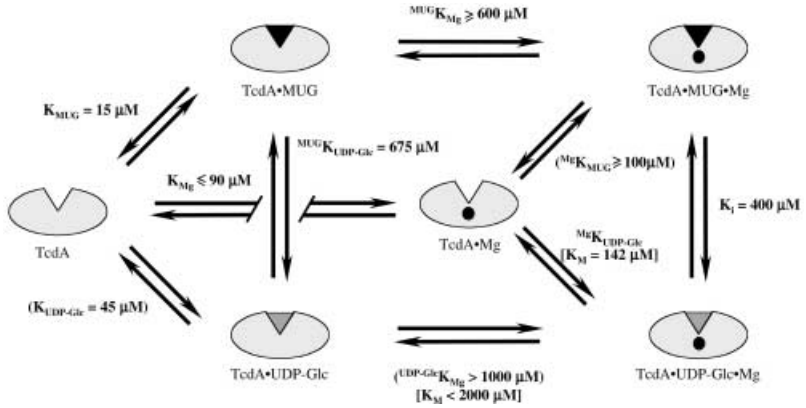

Fig. 5. Diagram showing the thermodynamic equilibria and their dissociation constants involved in the binding of UDP-Glc, MUG and Mg^{2+} to TcdA. Values shown in parentheses have been obtained by using the thermodynamic cycle and the equilibrium constants that could be readily measured using inhibition assays or fluorescence properties of MUG. Values in square brackets were measured in the kinetic studies of Ciesla & Bobak [11]. Values with neither parentheses nor brackets have been measured directly in these studies.

chemistry. All of the structures mentioned above have small water-filled cavities adjacent to the 2′-OH of the crystallographically observed UDP (or UDP-galactose in the case of LgtC), and hence might accommodate the methylanthraniloyl modified substrate analog with only minor rearrangements. To check this finding, 2′-MUG was computationally docked into the active sites of LgtC and BGT by using the program AUTODOCK [35] followed by simulated annealing. Little shift in the side chain positions (0.6 Å rmsd for LgtC and 0.4 Å rmsd for BGT) was observed. Very similar to the BGT-UDP crystal structure, the phosphodiester moiety of MUG makes several good hydrogen bonding interactions with positively charged arginine groups (R191, R195 and R269) in the minimized structure, thereby stabilizing the negative charge of MUG. The Mg^{2+} ions in the active site of TcdA might easily take the place of these basic residues in the stabilization of the enzyme–substrate complex.

Recent studies of substrate and metal binding to T4 BGT show significant structural changes upon UDP/UDP-Glc binding [33]. Addition of the Mg^{2+} or Mn^{2+} cofactor, on the other hand, induced only minor structural shifts despite the requirement of this cofactor for activity. These structural studies suggested that the main role of the metal cofactor was for the stabilization of an oxocarbonium ion intermediate. Whereas this activity may be part of the mechanistic role of the metal ion, it cannot be the entire story. We have shown that Mg^{2+} binding alters the affinity of the enzyme for the UDP-Glc substrate. If the role of this ion were only in the transition state, this coupled binding would not be observed. The role of Mg^{2+} in this reaction therefore must also involve stabilization of the enzyme–substrate complex. The location of the metal ion cofactor with respect to the nucleotide-sugar substrate varies in these structures. Most commonly, it is observed bridging the α- and β-phosphoryl oxygen atoms of UDP or UDP-Glc [30,31,36]. This mode of interaction is analogous to that observed in many Enzyme–Mg–ATP complexes. In the case of BGT, however, the Mg^{2+} ion only interacts with the β-phosphate. In each case, additional ligation to the metal is provided by amino-acid side-chains such as those of the DXD motif [17,37,38]. Continuing structural studies coupled with biophysical and enzymatic analysis of these enzymes should continue to improve our picture of how these glucosyl transfer reactions occur and the role that the metal ion cofactors play in stimulating this chemistry.

CONCLUSIONS

We have prepared a fluorescent analog of UDP-Glc and used it as a spectroscopic probe to investigate the mechanism of glucosyltransfer catalyzed by *C. difficile* toxin A. This substrate analog binds competitively with respect to the natural substrate but cannot be turned over by the toxin. We have been able to probe the binding of both the synthetic as well as the natural substrate through our assays and have shown significant coupling between the binding of UDP-Glc and the Mg^{2+} cofactor. This finding implies that one of the roles of this ion may be to stabilize the TcdA–UDP-Glc complex prior to formation of any mechanistic intermediates, such as an oxocarbonium ion, that might lie along the reaction coordinate for glucosyltransfer.

ACKNOWLEDGEMENTS

This work was generously supported by the Indiana University College of Arts and Sciences and a grant to A. L. F. from the American Chemical Society-Petroleum Research Fund (#35517-G4). A. K. was a summer REU student supported by the site grant DBI-9987835 from the National Science Foundation. We would like to thank Peter Mikulecky for helpful comments on the manuscript.

REFERENCES

1. Bartlett, J.G., Chang, T.W., Moon, N. & Onderdonk, A.B. (1978) Antibiotic-induced lethal enterocolitis in hamsters: studies with eleven agents and evidence to support the pathogenic role of toxin-producing *Clostridia*. *Am. J Vet Res*. **39**, 1525–1530.
2. Bartlett, J.G., Moon, N., Chang, T.W., Taylor, N. & Onderdonk, A.B. (1978) Role of *Clostridium difficile* in antibiotic-associated pseudomembranous colitis. *Gastroenterology* **75**, 778–782.
3. Jones, R.L. (2000) Clostridial enterocolitis. *Vet Clin. North Am. Equine Pract*. **16**, 471–485.
4. Itoh, K., Lee, W.K., Kawamura, H., Mitsuoka, T. & Magaribuchi, T. (1987) Intestinal bacteria antagonistic to *Clostridium difficile* in mice. *Lab. Anim*. **21**, 20–25.
5. Wilkins, T., Krivan, H., Stiles, B., Carman, R. & Lyerly, D. (1985) Clostridial toxins active locally in the gastrointestinal tract. *Ciba Found. Symp*. **112**, 230–241.
6. Just, I., Wilm, M., Selzer, J., Rex, G., von Eichel-Streiber, C., Mann, M. & Aktories, K. (1995) The enterotoxin from *Clostridium difficile* (ToxA) monoglucosylates the Rho proteins. *J. Biol. Chem*. **270**, 13932–13936.
7. Just, I., Selzer, J., Wilm, M., von Eichel-Streiber, C., Mann, M. & Aktories, K. (1995) Glucosylation of Rho proteins by *Clostridium difficile* toxin B. *Nature* **375**, 500–503.
8. Herrmann, C., Ahmadian, M.R., Hofmann, F. & Just, I. (1998) Functional consequences of monoglucosylation of Ha-Ras at effector domain amino acid threonine 35. *J. Biol. Chem*. **273**, 16134–16139.
9. Hippenstiel, S., Tannert-Otto, S., Vollrath, N., Krull, M., Just, I., Aktories, K., von Eichel-Streiber, C. & Suttorp, N. (1997) Glucosylation of small GTP-binding Rho proteins disrupts endothelial barrier function. *Am. J. Physiol*. **272**, L38–L43.
10. Chaves-Olarte, E., Florin, I., Boquet, P., Popoff, M., von Eichel-Streiber, C. & Thelestam, M. (1996) UDP-glucose deficiency in a mutant cell line protects against glucosyltransferase toxins from *Clostridium difficile* and *Clostridium sordellii*. *J. Biol. Chem*. **271**, 6925–6932.
11. Ciesla, W.P. Jr & Bobak, D.A. (1998) *Clostridium difficile* toxins A and B are cation-dependent UDP-glucose hydrolases with differing catalytic activities. *J. Biol. Chem*. **273**, 16021–16026.
12. Moncrief, J.S., Lyerly, D.M. & Wilkins, T.D. (1997) Molecular biology of the *Clostridium difficile* toxins. *The Clostridia: Molecular Biology and Pathogenesis* (Rood, J.I., McClane, B.A., Songer, J.G. & Titball, R.W., eds), pp. 369–392. Academic Press, New York.
13. Aktories, K., Selzer, J., Hofmann, F. & Just, I. (1997) Molecular mechanism of action of *Clostridium difficile* toxins A and B. *The Clostridia: Molecular Biology and Pathogenesis* (Rood, J.I., McClane, B.A., Songer, J.G. & Titball, R.W., eds), Academic Press, New York.
14. Faust, C., Ye. B. & Song, K.P. (1998) The enzymatic domain of *Clostridium difficile* toxin A is located within its N-terminal region. *Biochem. Biophys. Res. Commun*. **251**, 100–105.
15. Just, I. & Boquet, P. (2000) Large clostridial cytotoxins as tools in cell biology. *Curr. Top Microbiol Immunol*. **250**, 97–107.
16. Busch, C., Schomig, K., Hofmann, F. & Aktories, K. (2000) Characterization of the catalytic domain of *Clostridium novyi* alpha-toxin. *Infect. Immun*. **68**, 6378–6383.

17. Busch, C., Hofmann, F., Selzer, J., Munro, S., Jeckel, D. & Aktories, K. (1998) A common motif of eukaryotic glycosyltransferases is essential for the enzyme activity of large clostridial cytotoxins. *J. Biol. Chem.* **273**, 19566–19572.
18. Hendrickson, T.L. & Imperiali, B. (1995) Metal ion dependence of oligosaccharyl transferase: implications for catalysis. *Biochemistry* **34**, 9444–9450.
19. Zheng, Y., Glaven, J.A., Wu, W.J. & Cerione, R.A. (1996) Phosphatidylinositol 4,5-bisphosphate provides an alternative to guanine nucleotide exchange factors by stimulating the dissociation of GDP from Cdc42Hs. *J. Biol. Chem.* **271**, 23815–23819.
20. Kim, K.-B., Behrman, E.C., Cottrell, C.E. & Behrman, E.J. (2000) On the conformation of UDP-Glc, a sugar nucleotide. *J. Chem Soc. Perkin Transactions* **II**, 677–682.
21. Jameson, D.M. & Eccleston, J.F. (1997) Fluorescent nucleotide analogs: synthesis and application. *Fluorescence Spectroscopy* (Brand, L. & Johnson, M.L., eds), pp. 363–390. Academic Press, San Diego.
22. Jameson, D.M. & Sawyer, W.H. (1995) Fluorescence anisotropy applied to biomolecular interactions. *Methods Enzymol.* **246**, 283–300.
23. Jameson, D.M. & Eccleston, J.F. (1997) Fluorescent nucleotide analogs: synthesis and applications. *Methods Enzymol.* **278**, 363–390.
24. Cremo, C.R., Neuron, J.M. & Yount, R.G. (1990) Interaction of myosin subfragment 1 with fluorescent ribose-modified nucleotides. A comparison of vanadate trapping and SH1–SH2 cross-linking. *Biochemistry* **29**, 3309–3319.
25. Rensland, H., Lautwein, A., Wittinghofer, A. & Goody, R.S. (1991) Is there a rate-limiting step before GTP cleavage by H-ras p21? *Biochemistry* **30**, 11181–11185.
26. Moore, K.J., Webb, M.R. & Eccleston, J.F. (1993) Mechanism of GTP hydrolysis by p21N-ras catalyzed by GAP: studies with a fluorescent GTP analogue. *Biochemistry* **32**, 7451–7459.
27. Cheng, J.-Q., Jiang, W. & Hackney, D.D. (1998) Interaction of mant-adenosine nucleotides and magnesium with kinesin. *Biochemistry* **37**, 5288–5295.
28. Busch, C., Hofmann, F., Gerhard, R. & Aktories, K. (2000) Involvement of a conserved tryptophan residue in the UDP-glucose binding of large clostridial cytotoxin glycosyltransferases. *J. Biol. Chem.* **275**, 13228–13234.
29. Feig, A.L. (2000) The use of manganese as a probe for elucidating the role of magnesium ions in ribozymes. In *Metal Ions in Biological Systems*, *Vol. 37*: Manganese and its Role in Biological Processes (Sigel, H., & Sigel, A., eds) pp. 157–182. Marcel Dekker, New York.
30. Charnock, S.J. & Davies, G.J. (1999) Structure of the nucleotide-diphospho-sugar transferase, SpsA from *Bacillus subtilis*, in native and nucleotide-complexed forms. *Biochemistry* **38**, 6380–6385.
31. Persson, K., Ly, H.D., Dieckelmann, M., Wakarchuk, W.W., Withers, S.G. & Strynadka, N.C. (2001) Crystal structure of the retaining galactosyltransferase LgtC from *Neisseria meningitidis* in complex with donor and acceptor sugar analogs. *Nat. Struct. Biol.* **8**, 166–175.
32. Morera, S., Imberty, A., Aschke-Sonnenborn, U., Ruger, W. & Freemont, P.S. (1999) T4 phage beta-glucosyltransferase: substrate binding and proposed catalytic mechanism. *J. Mol. Biol.* **292**, 717–730.
33. Morera, S., Lariviere, L., Kurzeck, J., Aschke-Sonnenborn, U., Freemont, P.S., Janin, J. & Ruger, W. (2001) High resolution crystal structures of T4 phage beta- glucosyltransferase: induced fit and effect of substrate and metal binding. *J. Mol. Biol.* **311**, 569–577.
34. Boix, E., Swaminathan, G.J., Zhang, Y., Natesh, R., Brew, K. & Acharya, K.R. (2001) Structure of UDP complex of UDP-galactose: beta-galactoside-alpha-1,3-galactosyltransferase at 1.53-Å resolution reveals a conformational change in the catalytically important C terminus. *J. Biol. Chem.* **276**, 48608–48614.
35. Morris, G.M., Goodsell, D.S., Halliday, R.S., Huey, R., Hart, W.E., Belew, R.K. & Olson, A.J. (1998) Automated docking using a Lamarckian genetic algorithm and emperical binding free energy function. *J. Comput. Chem.* **19**, 1639–1662.
36. Unligil, U.M., Zhou, S., Yuwaraj, S., Sarkar, M., Schachter, H. & Rini, J.M. (2000) X-ray crystal structure of rabbit *N*-acetylglucosaminyltransferase I: catalytic mechanism and a new protein superfamily. *EMBO J.* **19**, 5269–5280.
37. Griffiths, G., Cook, N.J., Gottfridson, E., Lind, T., Lidholt, K. & Roberts, I.S. (1998) Characterization of the glycosyltransferase enzyme from the *Escherichia coli* K5 capsule gene cluster and identification and characterization of the glucuronyl active site. *J. Biol. Chem.* **273**, 11752–11757.
38. Wiggins, C.A. & Munro, S. (1998) Activity of the yeast MNN1 alpha-1,3-mannosyltransferase requires a motif conserved in many other families of glycosyltransferases. *Proc. Natl Acad. Sci. USA* **95**, 7945–7950.

SUPPLEMENTARY MATERIAL

The following material is available from http://www.blackwell-science.com/products/journals/suppmat/ejb/ejb3013/ejb3013sm.htm

Figure S1. Time course showing the glucosylhydrolase activity of the TcdA used in the biophysical studies.